

# The effect of the spin-orbit interaction on the band gap of half-metals

Ph. Mavropoulos, K. Sato, R. Zeller, and P. H. Dederichs  
*Institut für Festkörperforschung, Forschungszentrum Jülich, D-52425 Jülich, Germany*

V. Popescu and H. Ebert  
*Department Chemie/Physikalische Chemie, University of Munich,  
Butenandtstr. 5-13, D-81377 Munich, Germany*  
(Dated: November 2, 2018)

The spin-orbit interaction can cause a nonvanishing density of states (DOS) within the minority-spin band gap of half-metals around the Fermi level. We examine the magnitude of the effect in Heusler alloys, zinc-blende half metals and diluted magnetic semiconductors, using first-principles calculations. We find that the ratio of spin-down to spin-up DOS at the Fermi level can range from below 1% (e.g. 0.5% for NiMnSb) over several percents (4.2% for (Ga,Mn)As) to 13% for MnBi.

Half-metals are materials showing spin ferromagnetism, but with the exotic property of presenting a metallic density of states (DOS) only for the one spin direction (usually majority), in parallel with a clear band gap around the Fermi level  $E_F$  for the other direction. Experimentally, the first of the kind to be reported were half-metallic Heusler alloys by de Groot *et al.* in 1983.<sup>1</sup> More recently, other half-metals were found, such as  $\text{CrO}_2$ ,<sup>2</sup>  $\text{La}_{0.7}\text{Sr}_{0.3}\text{MnO}_3$ ,<sup>2</sup> or diluted magnetic semiconductors.<sup>3</sup> Furthermore, ordered zinc-blende CrAs and CrSb were fabricated by molecular beam epitaxy<sup>4</sup> and relevant calculations suggest these and many similar zinc-blende systems to be half-metallic.<sup>5,6</sup> So has been the case with a variety of Heusler alloys.<sup>7</sup> The rising interest in half-metallic systems is partly caused by their potential applications in spin electronics,<sup>8</sup> since junctions made of half-metals should theoretically present 100% magnetoresistance or 100% spin polarized currents.

Although the *ab-initio* calculations show the presence of half-metallicity in this variety of materials, with a clear band gap around  $E_F$  for the minority spin, this can be partly suppressed by, *e.g.*, defects,<sup>9</sup> spin excitations at increased temperature, or non-quasiparticle states.<sup>10</sup> Even at low temperature and in the defect-free case, there is still the question of spin-orbit interaction. Although this is weak and in many cases can be neglected, in principle it should couple the two spin channels so that the presence of states around  $E_F$  for the majority spin is partly reflected in the minority DOS. Thus one cannot have a real gap, but a small DOS, its smallness depending on the strength of the spin-orbit coupling for each material; this effect could have also implications in the ideas about spin-dependent transport and spintronics devices. It is the purpose of this paper to give a quantitative picture for this effect for a few typical systems, and to argue if and how crucially this could affect spin-dependent transport. As model systems we have chosen the Heusler alloy NiMnSb, the ordered zinc-blende alloys CrAs, CrSb and MnBi, and the chemical disorder in diluted magnetic semiconductor  $\text{Ga}_{0.95}\text{Mn}_{0.05}\text{As}$ .

Our first-principles calculations are based on the screened Korrington-Kohn-Rostoker (KKR) Green func-

tion method, incorporating fully relativistic effects (from where the spin-orbit interaction emerges). For the description of the diluted magnetic semiconductors, the coherent potential approximation (CPA) was also employed. Details about the method can be found in Ref. 11. In the calculations we have used the atomic sphere approximation (ASA), in which it is assumed that the potential around each atomic site is spherically symmetric. In the open structures, such as the zinc-blende, the large empty interstitial space is accounted for by placing at appropriate positions empty spheres (treated as atomic spheres with no nuclear charge). In the expansion of the Green function in local orbitals a cutoff of  $l_{\text{max}} = 3$  was taken for the ordered compounds and of  $l_{\text{max}} = 2$  for the CPA calculations. We have employed both the fully relativistic (solving the Dirac equation) and the scalar relativistic<sup>12</sup> methods for comparison. The latter includes all other relativistic effects except spin-orbit coupling, so that the two spin channels are decoupled and half-metals appear with a clean gap for spin-down around  $E_F$ .

The DOS  $n_\sigma(E)$  per spin  $\sigma$  is related to the retarded Green function  $G_\sigma(\vec{r}, \vec{r}'; E)$  via

$$n_\sigma(E) = -\frac{1}{\pi} \text{Im} \int G_\sigma(\vec{r}, \vec{r}; E) d^3r \quad (1)$$

Usually for the calculation a very small imaginary part  $i\epsilon$  is added to the real energy  $E$  and the Green function and DOS are evaluated at  $E + i\epsilon$ . In this way the DOS of every eigenstate is no more a delta function of the energy but is rather smoothed via a Lorentzian broadening. This method has the advantage of needing fewer  $\vec{k}$  points for the integration in the Brillouin zone to obtain a smooth DOS, saving computational time. Nevertheless there is the disadvantage that, in the presence of a band gap, the band edges are not sharp and one also obtains a very low nonzero DOS within the gap due to the Lorentzian broadening. In our case this causes a problem, since the DOS within the minority gap due to spin-orbit coupling is also small and drowned in the background of the Lorentzian broadening. To overcome this difficulty one would have to go much closer to the real energy axis, which would

demand too many  $\vec{k}$  points. We have used an alternative, which saves calculation time: Since the Green function is analytical in the complex energy plane  $E_z$ , we are able to extrapolate to the real energy axis by knowing the variation of the Green function for  $E_z$  along a line parallel to the real axis. To our knowledge, this method was first proposed by Gray and Kaplan,<sup>13</sup> who also report on the numerical limitations. The resulting accuracy within the gap is much better than that of the traditional method, and good enough for our purposes, although sometimes numerical fluctuations of the DOS are visible.

In our calculations we solve the Dirac equation, thus treating the spin-orbit term exactly. But for a better understanding we give now a brief description of the first order effect of the interaction in a Schrödinger picture. We remind that the spin-orbit coupling of the two spin channels is related to the unperturbed potential  $V(r)$  around each atom via the angular momentum operator  $\vec{L}$  and the Pauli spin matrix  $\vec{\sigma}$ :

$$V_{\text{so}}(r) = \frac{1}{2m^2c^2} \frac{\hbar}{2} \frac{1}{r} \frac{dV}{dr} \vec{L} \cdot \vec{\sigma} = \begin{pmatrix} V_{\text{so}}^{\uparrow\uparrow} & V_{\text{so}}^{\uparrow\downarrow} \\ V_{\text{so}}^{\downarrow\uparrow} & V_{\text{so}}^{\downarrow\downarrow} \end{pmatrix} \quad (2)$$

Analyzed in spinor basis, it takes the  $2 \times 2$  matrix form above. We denote the two spin directions with  $\uparrow$  and  $\downarrow$ , the unperturbed crystal hamiltonian for the two spin directions as  $H^{0\uparrow}$  and  $H^{0\downarrow}$ , and the unperturbed Bloch eigenfunctions as  $\Psi_{n\vec{k}}^{0\uparrow}$  and  $\Psi_{n\vec{k}}^{0\downarrow}$ . Then the Schrödinger equation for the perturbed wavefunction  $\Psi_{n\vec{k}} = (\Psi_{n\vec{k}}^{\uparrow}, \Psi_{n\vec{k}}^{\downarrow})$  reads

$$\begin{pmatrix} H^{0\uparrow} + V_{\text{so}}^{\uparrow\uparrow} - E & V_{\text{so}}^{\uparrow\downarrow} \\ V_{\text{so}}^{\downarrow\uparrow} & H^{0\downarrow} + V_{\text{so}}^{\downarrow\downarrow} - E \end{pmatrix} \begin{pmatrix} \Psi_{n\vec{k}}^{\uparrow} \\ \Psi_{n\vec{k}}^{\downarrow} \end{pmatrix} = 0 \quad (3)$$

The potential terms  $V_{\text{so}}^{\uparrow\downarrow}$  and  $V_{\text{so}}^{\downarrow\uparrow}$  are responsible for flipping the spin. Within the gap region of the half-metal, where no spin-down states of the unperturbed hamiltonian exist, the spin-down solution can be found in first order by solving Eq. (3) for  $\Psi_{n\vec{k}}^{(1)\downarrow}$  (the index (1) stands for the first-order solution). The solution reads formally:

$$\Psi_{n\vec{k}}^{(1)\downarrow} = -\frac{1}{H^{\downarrow} + V_{\text{so}}^{\downarrow\downarrow} - E_{n\vec{k}}^{0\uparrow}} V_{\text{so}}^{\downarrow\uparrow} \Psi_{n\vec{k}}^{0\uparrow} \quad (4)$$

with  $E_{n\vec{k}}^{0\uparrow}$  the eigenenergy of the state  $\Psi_{n\vec{k}}^{0\uparrow}$ . We see that in the gap region the spin-down intensity is a weak image of the band structure  $E_{n\vec{k}}^{0\uparrow}$  of the spin-up band. Since the DOS is related to  $|\Psi_{n\vec{k}}^{(1)\downarrow}|^2$ , it is expected that within the gap the DOS has a quadratic dependence on the spin-orbit coupling strength:  $n_{\downarrow}(E) \sim (V_{\text{so}}^{\downarrow\uparrow})^2$ . But there is also a modification by the term  $-1/(H^{\downarrow} + V_{\text{so}}^{\downarrow\downarrow} - E_{n\vec{k}}^{0\uparrow})$  (this is actually the Green function), which increases the weight of the states close to those  $\vec{k}$  points where the unperturbed spin-up and spin-down bands cross, *i.e.*,

$E_{n\vec{k}}^{0\uparrow} = E_{n'\vec{k}'}^{0\downarrow}$ . To see this we can rewrite Eq. (4) by expanding the Green function in spectral representation:

$$\begin{aligned} \Psi_{n\vec{k}}^{(1)\downarrow}(\vec{r}) &= \int d^3r' \sum_{n'} \frac{\Psi_{n'\vec{k}'}^{(0)\downarrow}(\vec{r}) \Psi_{n'\vec{k}'}^{(0)\downarrow*}(\vec{r}')}{E_{n\vec{k}}^{0\uparrow} - E_{n'\vec{k}'}^{0\downarrow}} V_{\text{so}}^{\downarrow\uparrow}(\vec{r}') \Psi_{n\vec{k}}^{(0)\uparrow}(\vec{r}') \\ &= \sum_{n'} \frac{\langle \Psi_{n'\vec{k}'}^{0\downarrow} | V_{\text{so}}^{\downarrow\uparrow} | \Psi_{n\vec{k}}^{0\uparrow} \rangle}{E_{n\vec{k}}^{0\uparrow} - E_{n'\vec{k}'}^{0\downarrow}} \Psi_{n'\vec{k}'}^{0\downarrow}(\vec{r}) \end{aligned} \quad (5)$$

Here, the summation runs only over the band index  $n'$  and not over the Bloch vectors  $\vec{k}'$ , because Bloch functions with  $\vec{k}' \neq \vec{k}$  are mutually orthogonal. Close to the crossing point  $E_{n\vec{k}}^{0\uparrow} - E_{n'\vec{k}'}^{0\downarrow}$  the denominator becomes small and the bands strongly couple. Then one should also consider higher orders in the perturbation expansion. Since at the gap edges there exist spin-down bands of the unperturbed hamiltonian, this effect can become important near the gap edges.

Now we proceed to the analysis of our results. The results for the Heusler alloy NiMnSb, which was found by de Groot *et al.* in 1983 to be half-metallic,<sup>1</sup> are shown in Fig. 1. In the top panel, the atom-resolved DOS is shown, following a scalar relativistic calculation. The Fermi level is within the band gap for minority spin and the material is half-metallic. In this scale, the relativistic calculation shows no difference in the DOS compared to the scalar relativistic. In the middle panel the gap region is shown in a relativistic calculation. Again, no minority DOS is seen in this scale. But when we magnify the minority DOS in the lower panel, it becomes clear that the DOS is nonzero in the gap region — it is of the order of 0.5% of the majority DOS in the vicinity of  $E_F$ . We have checked the DOS in this scale for the scalar relativistic calculation and have found it to be zero, thus we conclude that we see here a spin-orbit effect and not an artificial Lorentzian broadening due to the imaginary part of the energy in the calculation. The fluctuations of the Mn DOS (full line) are due to numerical noise of the  $\vec{k}$  integration and extrapolation scheme, and mark its limit of accuracy.

The next example is the ordered half-metallic alloy CrAs in the zinc-blende structure. This was invented by Akinaga and co-workers<sup>4</sup> in 2000 and found to be half-metallic. Our results are presented in Fig. 2. In the top panel, the scalar relativistic atom-resolved DOS is shown. The Fermi level is within the minority-spin gap, close to the conduction band edge. (The latter is mainly of  $d$  character, containing the wavefunctions of the  $e_g$  subspace<sup>6</sup>). Focusing in the range of the gap, we can see the DOS in more detail in the middle panel in a relativistic calculation. Below  $-1$  eV one recognises the majority  $d$  states of  $e_g$  character.<sup>6</sup> Around  $-0.9$  eV the DOS has a minimum, as the  $e_g$  states end and the  $d$  states of  $t_{2g}$  character start, forming wide bands. In this scale no spin-orbit effect is visible in the minority gap. But if we focus further in energy (lower panel) it is clear that the structure of the majority DOS is reflected in the minority DOS: one can recognize the peak of the  $e_g$  states below

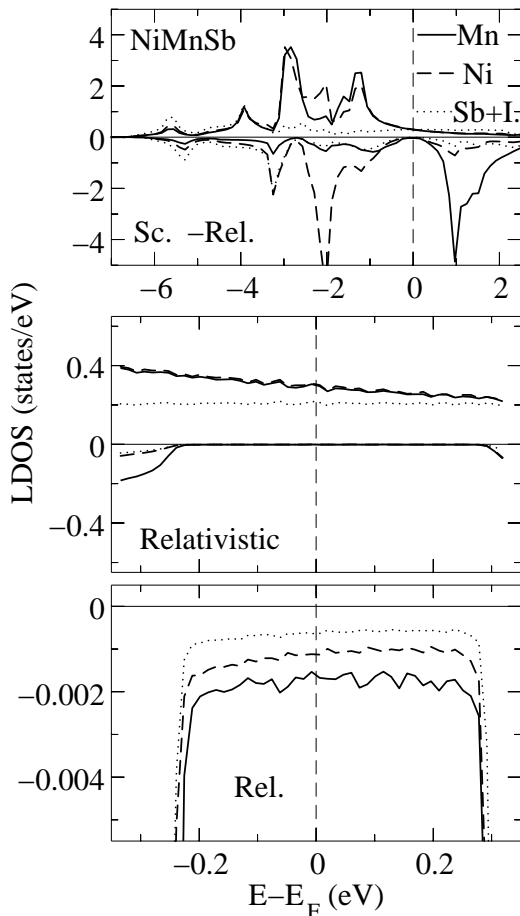


FIG. 1: DOS of NiMnSb. Top: scalar relativistic (I. refers to interstitial volume of the empty sphere). Middle: fully relativistic, focused in the minority-gap region around  $E_F$ . In this scale, the spin-orbit effect is not visible. Bottom: fully relativistic, focused on the minority states within the “gap”. The fluctuations reflect the numerical accuracy of the method (see text). Around  $E_F$ , the spin-down DOS is of the order of 0.5% of the spin-up DOS. Close to the “gap” edges, the spin-orbit induced minority DOS increases strongly as explained in the text. Negative numbers in the DOS axis correspond to minority spin.

-1 eV, then the minimum and finally the presence of the  $t_{2g}$  band above -0.8 eV. This is the effect of the term  $V_{so}^{\downarrow\uparrow}\Psi_{n\vec{k}}^{\uparrow}$  in Eq. (4). But we also observe the rapid increase of the DOS as the energy approaches the band edges; this comes from the term  $-1/(H^{\downarrow} + V_{so}^{\downarrow\downarrow} - E_{n\vec{k}}^{0\uparrow})$ . The minority DOS in the middle of the gap is again small, giving a minority/majority DOS ratio of 0.2%. In a similar calculation for zinc-blende CrSb (first fabricated by Zhao *et al.*<sup>14</sup>) we find that the minority DOS in the middle of the gap is around 0.7% of its majority counterpart. This rise is expected, as the spin-orbit interaction is stronger for the  $5p$  states of Sb than for the  $4p$  of As. (The trend can be seen for example in a systematic study of the

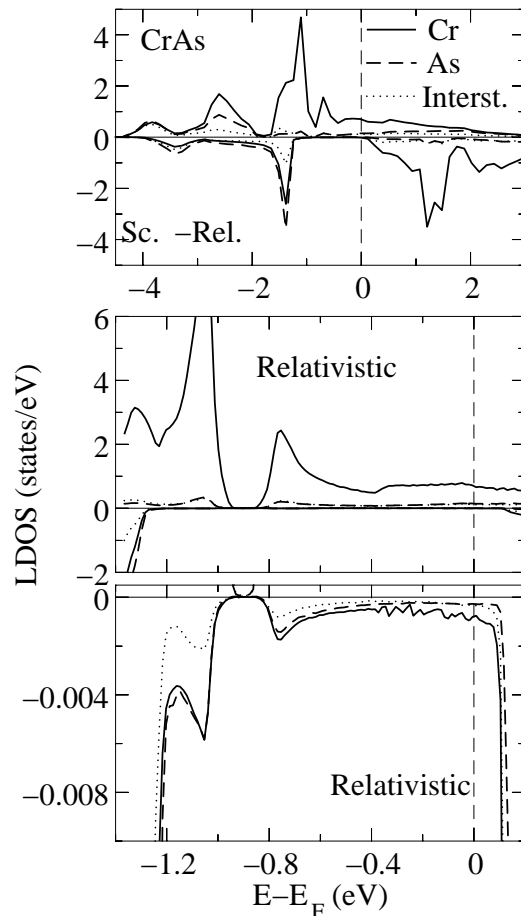


FIG. 2: DOS of zinc-blende CrAs. Top: scalar relativistic. Middle: fully relativistic, focused in the minority-gap region around  $E_F$ . In this scale, the spin-orbit effect is not visible. Bottom: fully relativistic, focused on the minority states within the “gap”. The reflection of spin-up into spin-down DOS is clear at the peaks at -1 eV and -0.8 eV. In the middle of the gap, the spin-down DOS is of the order of 0.2% of the spin-up DOS. Negative numbers in the DOS axis correspond to minority spin.

spin-orbit cross section of  $sp$  impurities in Mg in Ref. 15, where Sb is found to have four times higher spin-orbit cross section than As. Since the spin-orbit interaction is in first approximation an atomic property, the trend is similar here.)

A recent theoretical investigation<sup>16</sup> has suggested the ordered zinc-blende alloy MnBi as a good candidate for half-metallicity. Although this has not yet been fabricated, we take it as a good example to show the spin-orbit effect, since Bi is a heavy element with strong spin-orbit interaction because of the  $6p$  states. The scalar and fully relativistic DOS are shown in Fig. 3. It is evident that here the spin-orbit interaction has a much stronger influence. The minority DOS at  $E_F$  is of the order of 13% of its majority counterpart, a huge quantity in comparison to the analogous percentage in CrAs or NiMnSb. The

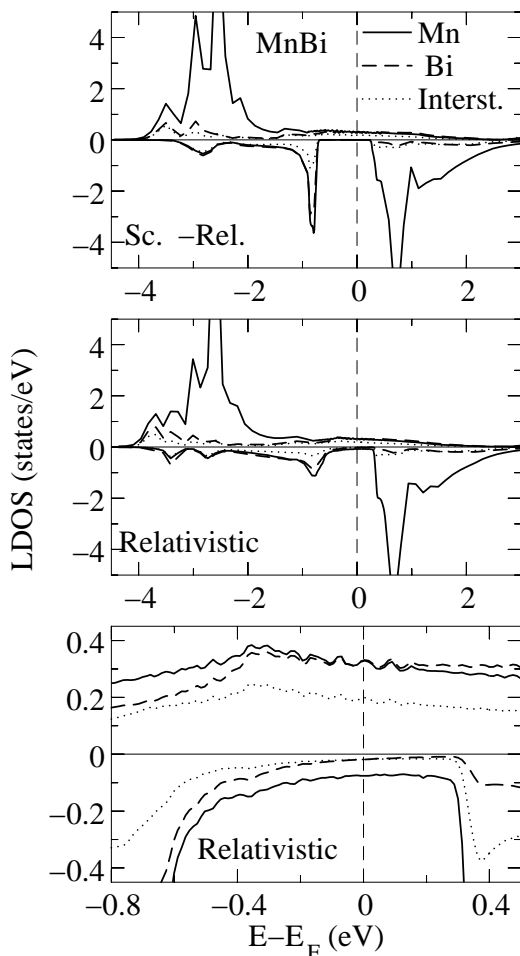


FIG. 3: DOS of zinc-blende MnBi. Top: scalar relativistic. Middle: Fully relativistic. Bottom: fully relativistic, focused on the states within the minority “gap”. At  $E_F$ , the spin-down DOS is of the order of 13% of the spin-up DOS. This higher value is expected since the  $6p$  valence states of Bi result in a strong spin-orbit effect. Negative numbers in the DOS axis correspond to minority spin.

relativistic effect shows up also in the orbital magnetic moment, being  $0.11\mu_B$  and mostly concentrated at the Mn atom, while the spin moment remains at  $4.0\mu_B$  per unit cell as in the scalar and non-relativistic case. We note that, although the spin-orbit interaction is strong here, the majority spin is still dominating at  $E_F$ . Thus MnBi would be a useful material for spin electronics despite the spin-orbit effect, as its spin polarization at  $E_F$  is robust against moderate volume change as pointed out in Ref. 16.

As a final example we consider the diluted magnetic semiconductor (DMS)  $\text{Ga}_{0.95}\text{Mn}_{0.05}\text{As}$ . This material, together with other similar DMS, has been extensively studied in recent years, because it presents ferromagnetism at such low Mn concentrations (discovered by Ohno<sup>3</sup> in 1998). Ideally, the Mn impurities substitute

Ga atoms in the GaAs lattice. Then the Mn  $3d$  states of the  $t_{2g}$  representation ( $d_{xy}$ ,  $d_{yz}$ , and  $d_{xz}$ ) hybridize with the  $p$  states of the As neighbors, forming bonding and antibonding  $p-d$  hybrids and from them states within the GaAs gap for the spin-up direction. Thus the alloy becomes half-metallic with  $E_F$  close to the valence band edge. Although there is no consensus yet on the physical origin of the ferromagnetic ordering, which seems to depend on the energetic position of the Mn  $d$  states,<sup>17</sup> we have proceeded using the LDA result. We find that the spin-down DOS at  $E_F$  is 4.2% of its spin-up counterpart if we include spin-orbit effects, while the system is half-metallic in the nonrelativistic solution. To understand this relatively high percentage of spin-down states, we observe that  $E_F$  is very close to the valence band edge. There, the  $p$  states of As give an important spin-orbit effect. This is known to split the valence band edge of GaAs in two subspaces, one with total (spin + orbital) angular momentum  $j = 3/2$  and one with  $j = 1/2$ , so that the valence band edge has no pure spin character.<sup>18</sup> Similar calculations on Mn-doped ferromagnetic zinc-blende GaN gave us no spin-orbit effect at  $E_F$  within numerical accuracy. The difference to (Ga,Mn)As is that the  $2p$  valence states of N compared to the  $4p$  of As (i) have a much lower spin-orbit interaction, and (ii) are lower in energy so that the Mn impurity  $d$  band is fully within the band gap, away from the N-dominated valence band states, and the spin-orbit effect weakens.

In summary, we have performed first-principles calculations in order to investigate the effect of the spin-orbit coupling to the spin-down band gap of half-metallic systems. As typical half-metallic systems, describable by the LDA, we have chosen the Heusler alloy NiMnSb, the ordered zinc-blende alloys CrAs, CrSb, and MnBi, and the diluted magnetic semiconductors (Ga,Mn)As and (Ga,Mn)N. We find that the majority-spin states are partly reflected into the minority band gap. The intensity of the DOS for minority electrons in this energy region depends mainly on the strength of the spin-orbit coupling, heavier  $sp$  elements resulting in a higher ratio of minority/majority spin DOS. Thus we see a trend of increasing min./maj. DOS ratio in the middle of the gap as we go from CrAs (0.2%) to CrSb (0.7%) and finally to MnBi (13%). In NiMnSb we find a ratio of 0.2%. Also, it is important how deep the Fermi level lies within the gap, since majority states close to the gap edges are more drastically spin-flipped than states deep in the gap. This results in high minority-spin DOS (4.2% ratio) for (Ga,Mn)As where  $E_F$  is very close to the valence band edge. We have also explained these effects within a first-order approximation. For transport applications in spintronics we conclude that even in compounds with strong spin-orbit effect (MnBi or (Ga,Mn)As) the minority DOS at  $E_F$  is still dominated by its majority counterpart (even in MnBi the ratio is only 13%), whence current should be transported practically only by majority states. Thus in applications other effects, such as gap states due to impurities,<sup>9</sup> stalking faults, or interfaces, could be more

important to eliminate by sample improvements.

### Acknowledgments

This work was supported by the RT Network of *Computational Magnetoelectronics* (contract RTN1-1999-

00145) of the European Commission. One of us (VP) gratefully acknowledges the financial support of the Deutsche Forschungsgemeinschaft withing the DFG-Förderprojekt FOG 370/2-1 "Ferromagnet-Halbleiter-Nanostrukturen: Transport, elektrische und magnetische Eigenschaften".

- 
- <sup>1</sup> R. A. de Groot, F. M. Mueller, P. G. van Engen, and K. H. J. Buschow, *Phys. Rev. Lett.* **50**, 2024 (1983).
- <sup>2</sup> R. J. Soulen *et al.*, *Science* **282**, 85 (1998).
- <sup>3</sup> H. Ohno, *Science* **281**, 951 (1998); F. Matsukura, H. Ohno, A. Shen, and Y. Sugawara, *Phys. Rev. B* **57**, R2037 (1998)
- <sup>4</sup> H. Akinaga, T. Manago, and M. Shirai, *Jpn. J. Appl. Phys.* **39**, L1118 (2000).
- <sup>5</sup> M. Shirai, *Physica E* **10**, 143 (2001); S. Sanvito and N. A. Hill, *Phys. Rev. B* **62**, 15553 (2000); A. Continenza *et al.*, *Phys. Rev. B* **64**, 085204 (2001); I. Galanakis, *Phys. Rev. B* **66**, 012406 (2002).
- <sup>6</sup> I. Galanakis and Ph. Mavropoulos, *Phys. Rev. B* **67**, 104417 (2003).
- <sup>7</sup> I. Galanakis, P. H. Dederichs, and N. Papanikolaou, *Phys. Rev. B* **66**, 134428 (2002); I. Galanakis, P. H. Dederichs, and N. Papanikolaou, *Phys. Rev. B* **66**, 174429 (2002).
- <sup>8</sup> S. A. Wolf *et al.*, *Science* **294**, 1488 (2001).
- <sup>9</sup> H. Ebert and G. Schütz, *J. Appl. Phys.* **69**, 4627 (1991).
- <sup>10</sup> V. Yu Irkhin and M. I. Katsnelson, *Physics-Uspeski* **37**, 659 (1994); V. Yu Irkhin and M. I. Katsnelson, *J. Phys.: Condens. Matter* **2**, 7151 (1990).
- <sup>11</sup> N. Papanikolaou, R. Zeller, and P. H. Dederichs, *J. Phys.: Condens. Matter* **14**, 2799 (2002); H. Ebert, in "Electronic Structure and Physical Properties of Solids", *Lecture Notes in Physics* vol. **535**, p. 191, edited by H. Dreyssé (Springer, Berlin 2000); H. Ebert, B. Drittler, and H. Akai, *J. Magn. Magn. Mater.* **104-107**, 733 (1992).
- <sup>12</sup> D. D. Koelling and B. N. Harmon, *J. Phys. C* **10**, 3107 (1977).
- <sup>13</sup> L. J. Gray and T. Kaplan, *J. Phys. A: Math. Gen.* **86**, 1555 (1986).
- <sup>14</sup> J. H. Zhao, F. Matsukura, K. Takamura, E. Abe, D. Chiba, and H. Ohno, *Appl. Phys. Lett.* **79**, 2776 (2001).
- <sup>15</sup> N. Papanikolaou, N. Stefanou, P. H. Dederichs, S. Geier, and G. Bergmann, *Phys. Rev. Lett.* **69**, 2110 (1992).
- <sup>16</sup> Y.-Q. Xu, B.-G. Liu, and D. G. Pettifor, *Phys. Rev. B* **66**, 184435 (2002).
- <sup>17</sup> Within the LDA, the Mn *d* states can be high in energy, close to  $E_F$ , whence the double-exchange mechanism dominates (H. Akai *Phys. Rev. Lett.* **81**, 3002 (1998); K. Sato, P. H. Dederichs, and H. Katayama-Yoshida, *Europhys. Lett.* **61**, 403 (2003)). But within the LDA+U the *d* states can be much lower, pushing up the As *p* states and the valence band (K. Sato, P. H. Dederichs, H. Katayama-Yoshida, and J. Kudrnovský, unpublished). This is suitable for investigation within *p-d* hamiltonian methods (T. Dietl *et al.*, *Science* **287**, 1019 (2000)).
- <sup>18</sup> Peter Y. Yu and Manuel Cardona, "Fundamentals of Semiconductors: Physics and Materials Properties", 3rd edition, Springer Verlag (2001)